NANO LETTERS

2005
Vol. 5, No. 7
1243−1246

# Basis and Lattice Polarization Mechanisms for Light Transmission through Nanohole Arrays in a Metal Film

**R. Gordon* and M. Hughes**

*Department of Elec. and Comp. Eng., University of Victoria, P.O. Box 3055, Victoria, Canada, V8W 3P6*

**B. Leathem and K. L. Kavanagh**

*Department of Physics, Simon Fraser University, 8888 University Drive, Burnaby, BC, Canada, V5A 1S6*

**A. G. Brolo**

*Department of Chemistry, University of Victoria, P.O. Box 3065, Victoria, BC, Canada, V8W 3V6*

*Received May 15, 2005*

**ABSTRACT**

**The extraordinary light transmission through double-hole and elliptical nanohole arrays in a thin gold film is investigated for different orientations of the holes relative to the lattice. Even though these bases have similar symmetry characteristics, the polarization follows the orientation of the basis for the ellipse but remains fixed along a lattice vector for the double holes. Furthermore, the maximum transmitted intensity for linearly polarized light is constant for the ellipse, but decreases for the double holes as they are rotated away from being aligned with the lattice. Finite-difference time-domain simulations agree well with the experimental findings. These experiments show how the basis determines both the coupling into the surface plasmon waves and the evanescent transmission through the nanoholes. Both of these effects need to be considered when designing nanophotonic devices using the extraordinary transmission phenomenon.**

Light transmission through subwavelength holes can be increased by several orders of magnitude with respect to Bethe's theory[1] when the holes are periodically arranged in a thin metal film.[2] This extraordinary transmission is the result of resonant coupling to surface plasmon (SP) waves at the metal−dielectric interface via the array of holes.[3,4,5,6,7] As with other periodic systems, the optical response of the hole array is determined by both the lattice and the basis. The SP waves are longitudinal, so the polarization is collinear with their direction of propagation.[8] This means that the polarization direction of the incident field selects which resonance of the lattice is excited. Recent works have shown that changing the basis shape from circular holes to elliptical[9,10] and rectangular[11] holes has a strong influence on the polarization and resonance properties; as the aspect ratio is increased, the polarization perpendicular to the broad edge of the hole has enhanced transmission and the resonance peaks shift in wavelength. Those works focused on the situation in which the elongated basis was aligned with the array's lattice vector. As a result, they did not separate the contributions of the basis and the lattice. Furthermore, both the ellipses and the rectangles considered in those works have a strongly polarized (evanescent) transmission mode through the holes, which was not distinguishable from the other polarization effects.

In this work, we investigate the effect of the array basis and its orientation on the transmission. By comparing the behavior of ellipses to double-hole arrays, the contributions of the lattice and basis are distinguished. When the ellipses and the double holes are aligned with the lattice, they both show enhanced transmission for light polarized perpendicular to their long axis. Upon rotation of the basis, however, the transmission of the ellipses and double holes have different polarization behaviors. These experimental results are in good agreement with theoretical simulations based on finite-difference time-domain (FDTD) calculations. They are

* Corresponding author. E-mail: rgordon@uvic.ca.

10.1021/nl0509069 CCC: $30.25 
**Published on Web 06/22/2005**

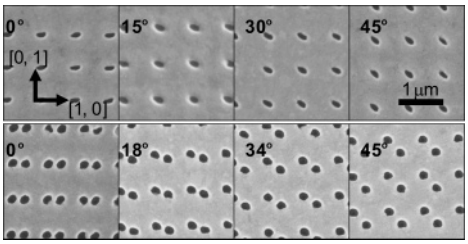


**Figure 1.** Scanning electron microscope image of elliptical and double-hole arrays fabricated in a gold film. The image was taken with secondary electron detection with a 5 kV bias. The double holes have a horizontal center-to-center spacing of 270 nm, and all of the arrays have a lattice constant of 710 nm. The [0, 1] and [1, 0] lattice vectors (for all the arrays) are shown with arrows in the top left image.

interpreted in terms of differences in the coupling between the incident plane wave and the SP modes and the effect of hole shape on the transmission through the evanescent mode of the metal layer.

The nanohole arrays were fabricated and imaged with a dual-beam focused ion beam and field-emission scanning-electron microscope. The gallium-ion beam was set to 30 keV with a milling rate of 1.6 nm/s for gold and a beam current of 300 pA. The typical resolution of the milling beam was 20 nm. The milling time was chosen to mill through the 100-nm-thick gold film, which was supported by a glass substrate. A 5-nm chromium layer was present to improve the adhesion of the gold film. The arrays were 25 $\mu$m$^2$, and the milling time was less than 1 min per array. Figure 1 shows the double-hole and ellipse arrays that were fabricated. The square lattice spacing was fixed at 710 nm for all of the arrays. The ellipses had a major axis length of 215 nm and a minor axis length of 95 nm. The orientation of the ellipses was changed from 0 to 45° in 15° increments. The aspect ratio of the ellipses was kept fixed for this work.

The double holes were fabricated with a fixed [1, 0] center-to-center displacement of 255 nm, while the [0, 1] displacement was varied in steps of 85 nm from 0 to 255 nm, with a corresponding rotation of the axis through the hole centers of 0, 18.4, 33.7, and 45°. This configuration was chosen to facilitate fabrication, and it means that the spacing between the holes changes in addition to the rotation. The diameter of each hole was 180 nm.

White light from a halogen bulb was collimated, polarized, and focused onto each array through the glass substrate at normal incidence using a 20× microscope objective. The spot size was several times larger than the arrays, so the illumination of the arrays may be considered constant. The transmitted light was collected with a broad-area fiber (400-$\mu$m core) located 1 cm from the sample and coupled into an optical spectrum analyzer. The collection point was verified to be at the zero of the transverse k-space (i.e., normal detection) by translating the fiber laterally to ensure that the spectrum varied in a symmetric manner about the central point.

Figure 2a and b shows the polarization-dependent transmission spectrum of ellipses and double holes. In this case, both the double holes and the ellipses were oriented along the [1, 0] lattice vector, as shown in the first SEM image of Figure 1 (0° orientation). The p-polarization lies normal to the major axis of the ellipse and normal to the axis joining the adjacent holes for the double-hole basis. The SP resonances from the gold-substrate side were suppressed by the 5-nm chromium adhesion layer,[12] which introduces strong losses to the SP modes. For this orientation, it is clear that the (0, 1) SP resonance for the gold−air interface, located at 790 nm, had the same polarization dependence for both the ellipses and the double holes: the resonance was enhanced for the p-polarization and absent for the s-polarization. The (1, 1) resonance was located at 610 nm.

To verify that the resonances we observed were not from localized SPs, we measured the dispersion in the wavelength of the resonances as a function of the transverse collection wave-vector. Figure 2c shows one of these dispersion measurements for the double-hole array shown in Figure 2b. These measurements were taken for normal incidence, and

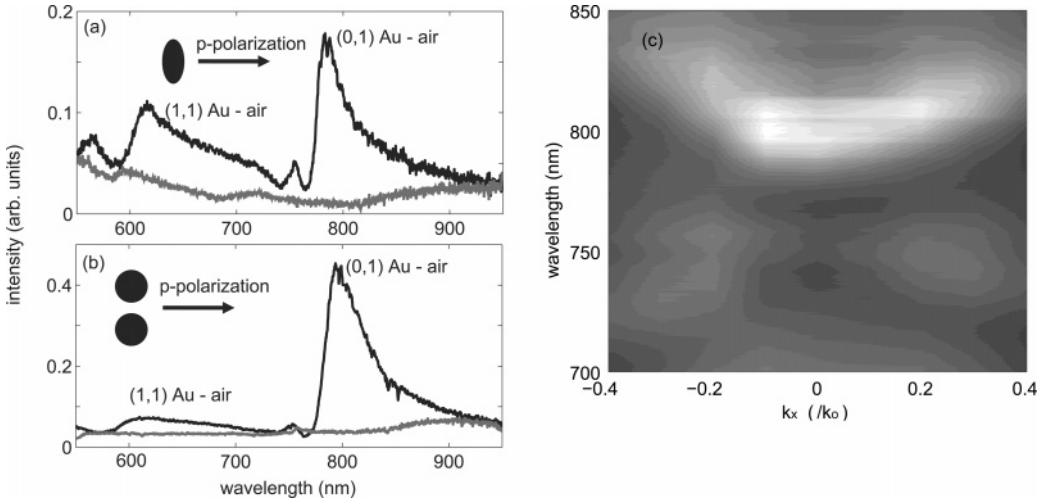


**Figure 2.** Normal transmission spectrum for the (a) ellipse and (b) double-hole basis arrays for polarization normal to the broad axis (p-polarization, black line) and parallel with the broad axis (s-polarization, gray line), as shown in the schematic insets. (c) Dispersion of wavelength as a function of the transverse wave-vector (normalized to the free-space wave-vector) as measured for the double-hole array.

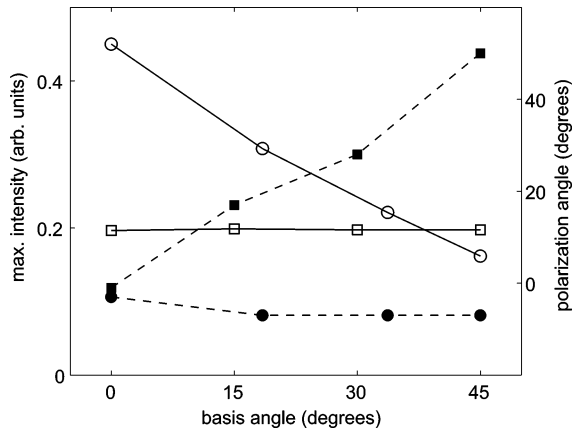


**Figure 3.** Experimentally observed maximum transmission intensity for the (1, 0) resonance. The solid lines show the maximum intensity (left axis) for the ellipses (open squares) and the double holes (open circles). The dashed lines show the polarization angle of maximum transmission (right axis) for the ellipses (filled squares) and double holes (filled circles).

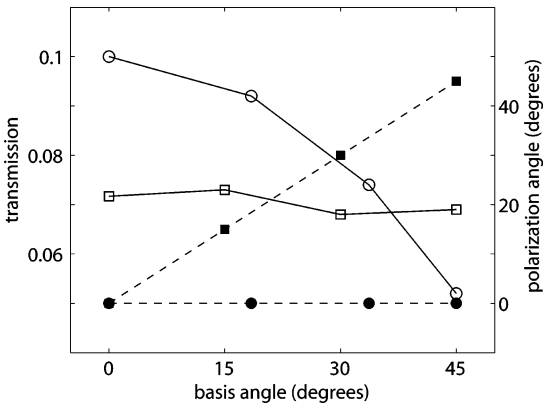


**Figure 4.** Finite-difference time-domain calculated transmission (as a fraction of the total incident power) for the (1, 0) resonance, for comparison with the experimental results in Figure 3. The solid lines show the maximum intensity (left axis) for the ellipses (open squares) and the double holes (open circles). The dashed lines show the polarization angle of maximum transmission (right axis) for the ellipses (filled squares) and double holes (filled circles).

the fiber was translated laterally to collect the transmitted light with a varying transverse wave-vector. A red shift was observed in the main resonance peak as the transverse wave-vector was increased. The measured dispersion curves were in agreement with extended SP polarizations, and not localized SPs, interacting with the array.[13] Furthermore, localized SPs associated with a single hole have a resonance that is typically several times broader than the ones observed here.[11,14]

Figure 3 shows the maximum transmitted (0, 1) intensity (left axis) and the polarization angle at the maximum intensity (right axis) for the ellipses and double holes, as a function of the array basis rotation angle. Different behavior was observed for the double holes and the ellipses. For the ellipses, the maximum transmission occurred when the light was polarized perpendicular to the major axis of the ellipse; as the ellipse is rotated, the polarization followed the ellipse orientation and not the lattice vector. For the double holes, the maximum transmission was polarized along the [1, 0] axis of the lattice for all orientations: the polarization followed the lattice and not the basis. The maximum transmitted intensity also showed different behavior for the two different bases. The ellipses had a constant maximum intensity for different basis orientations, whereas the double holes had a decreasing intensity. As the polarization of the incident light was rotated, the transmission at the resonance wavelength died down to a minimum value. That minimum value was the same for arrays with different orientations of the basis. These experiments show that the maximum polarization of transmission can follow the orientation of either the basis or the lattice, depending upon the shape of the basis chosen.

Recent experiments on single holes or holes in random arrays have shown that the shape of the single hole plays an important role in the transmission properties.[11,14] We have shown that SP coupling inside of the holes leads to a "shape effect".[15] That shape effect is localized to a single hole, so it cannot explain the lattice-dependent behavior that is observed here.

Figure 4 shows the FDTD simulation[16] results, which have good agreement with the experiments presented in Figure 3 for the same conditions. Periodic boundary conditions were used to model the lattice, with perfectly matched layers above and below the metal film to simulate the free propagation of light away from the surface. The response of the gold layer was captured using the standard Drude model.[17] Using a uniform 5-nm grid size, we integrated with 8.7 attosecond time-steps for a duration of 115 fs and calculated the resulting transmission. The resonance peak and polarization behavior was found to be in agreement with the experiments: the polarization followed the basis and the intensity was uniform for the ellipses, whereas the polarization followed the lattice and the intensity decreased for the double holes.

The physical origin of the observed behavior arises from the separate contributions of the lattice and basis to the enhanced transmission. The lattice is responsible for Bragg resonances in the SPs that allow for enhanced transmission. Obviously, these resonances are polarized along the lattice vectors. With the ellipse, the combined coupling to the (1, 0) and (0, 1) resonances is unchanged, whereas the coupling changes as the double holes are varied.

The basis alone also polarizes the light transmission because of the polarization-dependent transmission of the lowest-order evanescent mode of the hole. It has been shown that the lowest-order mode plays a dominant role in the transmission of the nanohole array.[5] The lowest-order mode for the ellipse is polarized with the electric field perpendicular to the major axis. The double holes, however, have a negligible polarization contribution to the evanescent modes because they are far enough apart to be treated as two separate circularly symmetric holes. (This has been verified with numerical simulations using MODE from Lumerical Solutions Inc.) Each circularly symmetric hole has no preferred polarization axis. It is clear that the polarization from the basis is dominating the transmission properties of the elliptical holes, whereas there is no such contribution for the double holes, so the polarization is from the lattice alone.

In conclusion, by investigating the extraordinary transmission of light through elliptical and double holes arranged periodically in a gold film, we have shown that the orientation and shape of the basis plays an important role in the polarization of the transmitted light through nanoholes. In particular, there are two polarizing effects that must be accounted for: (1) the coupling to the SP modes that enhance the amount of light coupled through the holes, and (2) the transmission through the holes. The understanding of these two separate effects will be important for designing nanohole devices for nonlinear optics and switching,[18,19] sensing and spectroscopy,[20−23] quantum information processing,[24] and near-field lithography.[25,26]

**Acknowledgment.** We acknowledge funding support from NSERC, CFI, and BCKDF. Collaboration was facilitated by CAMTEC, PCAMM, and CIPI.

## References

(1) Bethe, H. *Phys. Rev.* **1944**, *77*, 163−182.
(2) Ebbesen, T. W.; Lezec, H. J.; Ghaemi, H. F.; Thio, T.; Wolff, P. A. *Nature* **1998**, *391*, 667−669.
(3) Martìn-Moreno, L.; Garcìa-Vidal, F. J.; Lezec, H. J.; Pellerin, K. M.; Thio, T.; Pendry, J. B.; Ebbesen, T. W. *Phys. Rev. Lett.* **1998**, *86*, 1114−1117.
(4) Popov, E.; Neviere, M.; Enoch, S.; Reinisch, R. *Phys. Rev. B* **2000**, *62*, 16100−16108.
(5) Enoch, S.; Popov, E.; Neviere, M.; Reinisch, R. *J. Opt. A: Pure Appl. Opt.* **2002**, *4*, s83−s87.
(6) Barnes, W. L.; Murray, W. A.; Dintinger, J.; Devaux, E.; Ebbesen, T. W. *Phys. Rev. Lett.* **2004**, *92*, 107401.
(7) Sarrazin, M.; Vigneron, J.-P.; Vigoureux, J.-M. *Phys. Rev. B* **2003**, *67*, 085415.
(8) Raether, H. *Surface Plasmons;* Springer-Verlag: Berlin, 1988.
(9) Gordon, R.; Brolo, A. G.; McKinnon, A.; Rajora, A.; Leathem, B.; Kavanagh, K. L. *Phys. Rev. Lett.* **2004**, *92*, 037401.
(10) Azad, A. K.; Zhao, Y.; Zhang, W. *Appl. Phys. Lett.* **2005**, *86*, 141102.
(11) Koerkamp, K. J. K.; Enoch, S.; Segerink, F. B.; van Hulst, N. F.; Kuipers, L. *Phys. Rev. Lett.* **2004**, *92*, 183901.
(12) Genet, C.; van Exter, M.; Woerdman, J. *Opt. Commun.* **2003**, *225*, 331−336.
(13) Murray, W. A.; Astilean, S.; Barnes, W. L. *Phys. Rev. B* **2004**, *69*, 165407.
(14) Degiron, A.; Lezec, H. J.; Yamamoto, N.; Ebbesen, T. W. *Opt. Commun.* **2004**, *239*, 61−66.
(15) Gordon, R.; Brolo, A. G. *Opt. Express* **2005**, *13*, 1933−1938.
(16) Taflove, A.; Hagness, S. C. *Computational Electrodynamics: The Finite-Difference Time-Domain Method;* Artech House: Norwood, MA, 2000.
(17) Johnson, P. B.; Christy, R. W. *Phys. Rev. B* **1972**, *6*, 4370−4379.
(18) Nahata, A.; Linke, R. A.; Ishi, T.; Ohashi, K. *Opt. Lett.* **2003**, *28*, 423−425.
(19) Bigot, J.-Y.; Benabbas, A.; Degiron, A.; Ebbesen, T. W.; Guidoni, L.; Halté, V.; Lezec, H.; Saeta, P. *Quantum Electron. Laser Sci. (QELS), Postconf. Dig.* **2003**, 169.
(20) Liu, Y.; Blair, S. *Opt. Lett.* **2003**, *28*, 507−509.
(21) Brolo, A. G.; Gordon, R.; Leathem, B.; Kavanagh, K. L. *Langmuir* **2004**, *20*, 4813−4815.
(22) Sheehan, A. D.; Quinn, J.; Daly, S.; Dillon, P.; O'Kennedy, R. *Anal. Lett.* **2003**, *36*, 511−537.
(23) Brolo, A. G.; Arctander, E.; Gordon, R.; Leathem, B.; Kavanagh, K. L. *Nano Lett.* **2004**, *4*, 2015−2018.
(24) Altewischer, E.; van Exter, M. P.; Woerdman, J. P. *Nature* **2002**, *418*, 304−306.
(25) Shinada, S.; Hashizume, J.; Koyama, F. *Appl. Phys. Lett.* **2003**, *83*, 836−838.
(26) Srituravanich, W.; Fang, N.; Sun, C.; Luo, Q.; Zhang, X. *Nano Lett.* **2004**, *4*, 1085−1088.

NL0509069